

**Supplementary Information for**  
**Gate-controlled Magnetotransport and Electrostatic Modulation**  
**of**  
**Magnetism in 2D magnetic semiconductor CrPS<sub>4</sub>**

Fan Wu,<sup>1,2,\*</sup> Marco Gibertini,<sup>3,4</sup> Kenji Watanabe,<sup>5</sup> Takashi Taniguchi,<sup>6</sup>  
Ignacio Gutiérrez-Lezama,<sup>1,2</sup> Nicolas Ubrig,<sup>1,2,†</sup> and Alberto F. Morpurgo<sup>1,2,‡</sup>

<sup>1</sup>*Department of Quantum Matter Physics, University of Geneva,  
24 Quai Ernest Ansermet, CH-1211 Geneva, Switzerland*

<sup>2</sup>*Department of Applied Physics, University of Geneva,  
24 Quai Ernest Ansermet, CH-1211 Geneva, Switzerland*

<sup>3</sup>*Dipartimento di Scienze Fisiche, Informatiche e Matematiche,  
University of Modena and Reggio Emilia, IT-41125 Modena, Italy*

<sup>4</sup>*Centro S3, CNR Istituto Nanoscienze, IT-41125 Modena, Italy*

<sup>5</sup>*Research Center for Functional Materials, National Institute  
for Materials Science, 1-1 Namiki, Tsukuba 305-0044, Japan*

<sup>6</sup>*International Center for Materials Nanoarchitectonics, National  
Institute for Materials Science, 1-1 Namiki, Tsukuba 305-0044, Japan*

## CONTENTS

|                                                                 |   |
|-----------------------------------------------------------------|---|
| S1. Crystal characterization                                    | 2 |
| S2. Bias dependence of field effect mobility at low temperature | 3 |
| S3. Additional transport data                                   | 4 |
| References                                                      | 7 |

### S1. CRYSTAL CHARACTERIZATION

CrPS<sub>4</sub> single crystals were purchased from HQ Graphene, and the chemical composition and stoichiometry was confirmed by energy dispersive X-Ray spectroscopy (EDS) in a scanning electron microscope. The elemental mapping (Figure S1) confirms the uniform distribution of the elements, with an atomic ratio Cr:P:S of 16.92 : 16.60 : 66.48, in good agreement with the expected 1:1:4 stoichiometry.

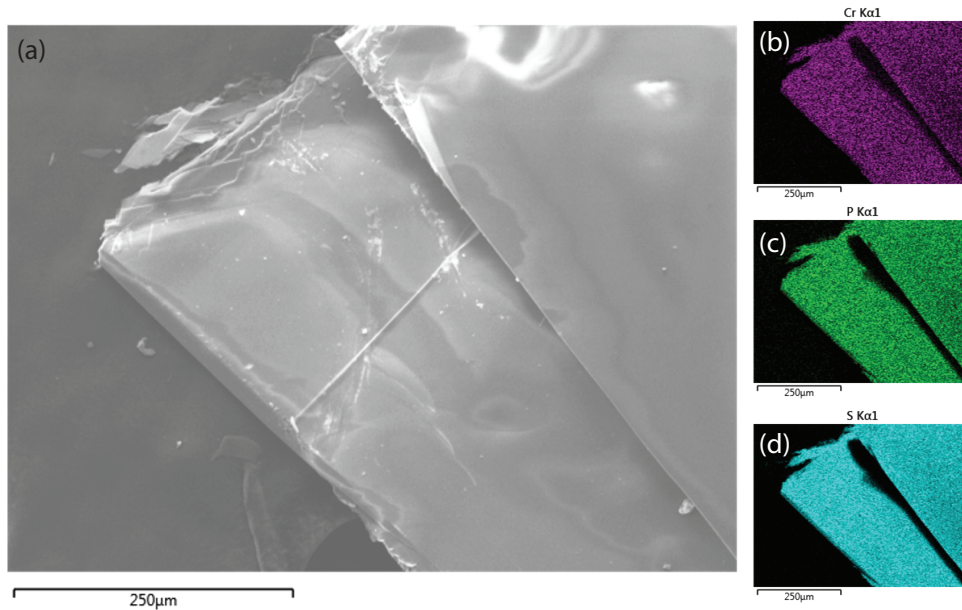


FIG. S1. (a) SEM image of the CrPS<sub>4</sub> single crystal employed in the EDS analysis. Elemental mapping of (b) Cr, (c) P and (d) S, resulting in an atomic ratio Cr:P:S of 16.92 : 16.60 : 66.48.

\* [fan.wu@unige.ch](mailto:fan.wu@unige.ch)

† [nicolas.ubrig@unige.ch](mailto:nicolas.ubrig@unige.ch)

‡ [alberto.morpurgo@unige.ch](mailto:alberto.morpurgo@unige.ch)

We also characterized our CrPS<sub>4</sub> crystals by Raman spectroscopy. Raman spectra were acquired by illuminating thin crystals exfoliated onto a SiO<sub>2</sub>/Si substrate with a 532 nm continuous wave laser (nominal power 60  $\mu$ W), and collecting the scattered light with a microscope objective. The scattered light was fed into a spectrometer equipped with a N<sub>2</sub> cooled Si charge coupled device array (LabRAM HR Evolution), enabling a resolution of the optical spectra of 0.3 cm<sup>-1</sup>. Figure S2 shows Raman spectrum measured on a 10 nm thick crystal, which is in good agreement with previously reported Raman measurements performed on few layers CrPS<sub>4</sub><sup>1,2</sup>.

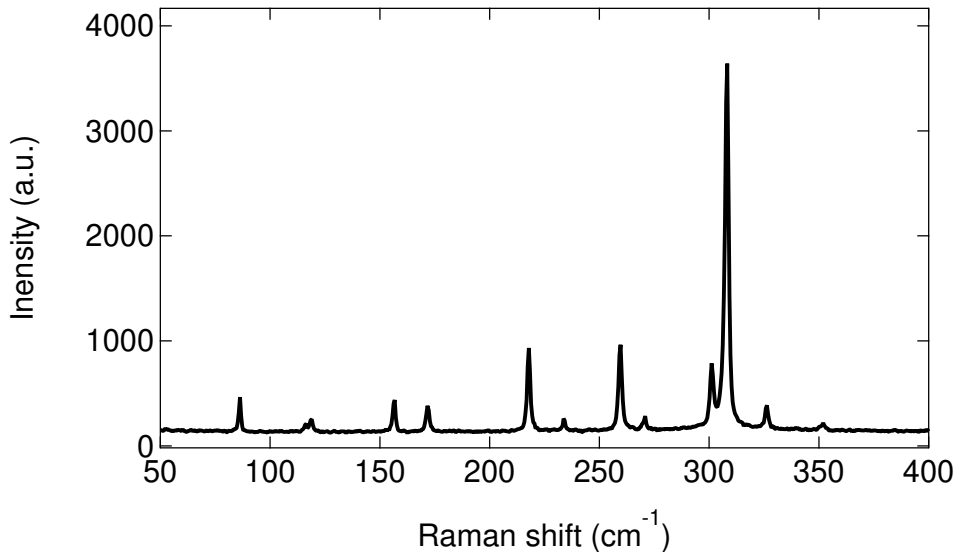


FIG. S2. Raman spectrum of a 10 nm CrPS<sub>4</sub> multilayer exfoliated on a SiO<sub>2</sub>/Si substrate.

## S2. BIAS DEPENDENCE OF FIELD EFFECT MOBILITY AT LOW TEMPERATURE

In the main text we argued that the influence of the contact resistance on the magneto-transport properties is negligible if a sufficiently large source-drain bias  $V_{SD}$  is applied. This argument is based on the fact that the mobility becomes independent of  $V_{SD}$  for sufficiently high biases. Here, we substantiate the claim with data measured at low temperature for device S2 in Fig. S3. Transfer curves of the transistor measured with  $V_{SD}$  ranging from 0.2 to 2 V are plotted in Fig. S3a. The field-effect mobility estimated from the slope of transconductance (see red linear fitting curves in Fig. S3a) increases with increasing  $V_{SD}$  up to  $V_{SD} \approx 1$  V

(see Fig. S3b), and saturates at a value of approximately  $4 \text{ cm}^2\text{V}^{-1}\text{s}^{-1}$ . This value is comparable to the mobility estimated from other reported 2D magnetic semiconductor like CrSBr and  $\text{NiI}_2$ , whose measurements were performed in a 4-terminal configuration<sup>3-5</sup>.

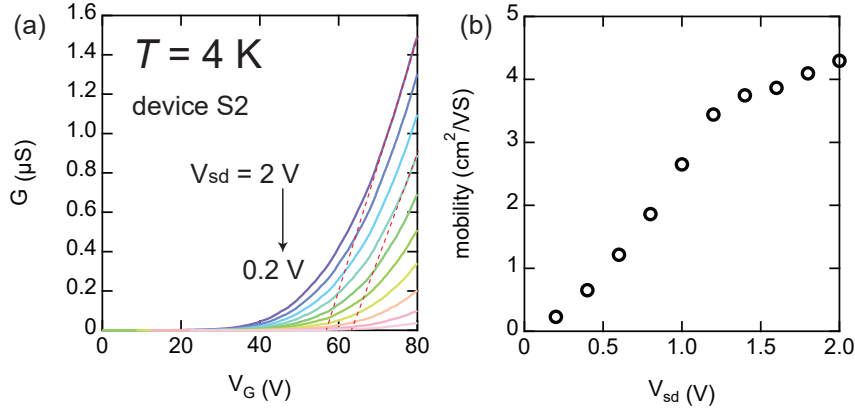


FIG. S3. (a) Transfer curves of device S2, based on a 9.7 nm thick  $\text{CrPS}_4$  multilayers, measured at 4 K for source-drain biases  $V_{\text{SD}}$  ranging from 0.2 to 2 V. (b) Field-effect mobility as a function of applied source-drain bias  $V_{\text{SD}}$ , showing that for voltages higher than 1.2 V the mobility becomes almost independent of the applied  $V_{\text{SD}}$ .

### S3. ADDITIONAL TRANSPORT DATA

Our work shows that transistors based on  $\text{CrPS}_4$  operate far below the *Néel* temperature and that we are able to tune the magnetic phase boundaries as a function of the gate voltage. In the main text, we illustrated these findings with data measured from a device made out of a 10 nm thick  $\text{CrPS}_4$  crystal, which are representative of the behavior of all devices measured. For completeness, we show here some of the key experimental observations, measured in the other devices that we have studied, as it is important to substantiate our claim regarding the reproducibility of the experimental results.

Fig. S4a-c shows the transfer curves of all other devices that have been investigated in our study (the thickness of  $\text{CrPS}_4$  multilayers ranges from 6 to 11 nm), measured at different temperature ranging from 50 K to 2 K. All transistors show a similar behavior to that of the device discussed in the main text. A finite low temperature conductance is observed upon applying positive voltages to the backgate. The threshold voltage and the field-effect

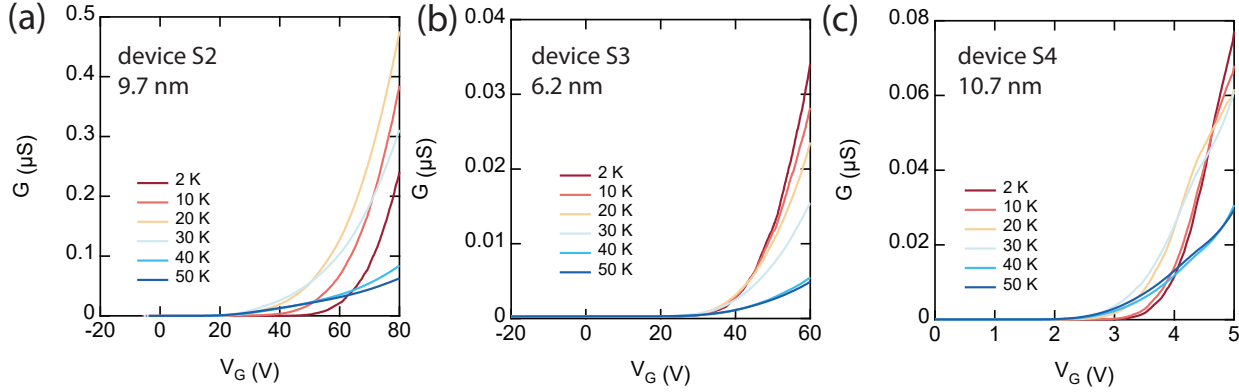


FIG. S4. Transfer curves of the different devices realized on (a) 9.7 nm, (b) 6.2 nm and (c) 10.7 nm thick  $\text{CrPS}_4$  multilayers (measurements are performed at selected temperatures between 50 and 2 K). For devices S2 and S3, the highly doped Silicon substrate is used as a gate with 285 nm thick  $\text{SiO}_2$  gate insulator; for device S4, a bottom graphene layer has been used as a back-gate electrode, and a 12 nm thick bottom h-BN crystal has been used as gate dielectric.

mobility varies between individual devices probably because of a slightly different doping level in different  $\text{CrPS}_4$  multilayers. Analogous to the device in the main text, decreasing temperature results in an increase of the threshold voltage. Irrespective of these details, these observations show that exfoliated crystals of  $\text{CrPS}_4$  are suitable for the systematic realization of FETs and operate properly down to cryogenic temperature.

Our magnetotransport measurements show that the magnetic phase boundaries of  $\text{CrPS}_4$  multilayers can be directly probed from the temperature and magnetic field dependence of the conductance. In Fig. S5 we present the detailed characterization of the magnetic phase diagram from transport measurements from a device which is distinct from the one discussed in the main text (labelled S2 in Fig. S4), which illustrate the reproducibility of our results. Identically to what we have shown in the main text, Fig. S5a shows a sharp conductance increase as the temperature is decreased below the onset of magnetic order. As shown in Fig. S5b, this device also exhibit a large magnetoconductance, approaching 8000 % at base temperature (the data was measured at  $V_G = +50 \text{ V}$ ). The magnetic phase diagram can be mapped by looking at  $dG/dH$ , as a function of temperature and magnetic field (see Fig. S5c). The *Néel* temperature at different gate voltages can be extracted by analyzing the derivative of the conductance as a function of the temperature (see Fig. S5d).

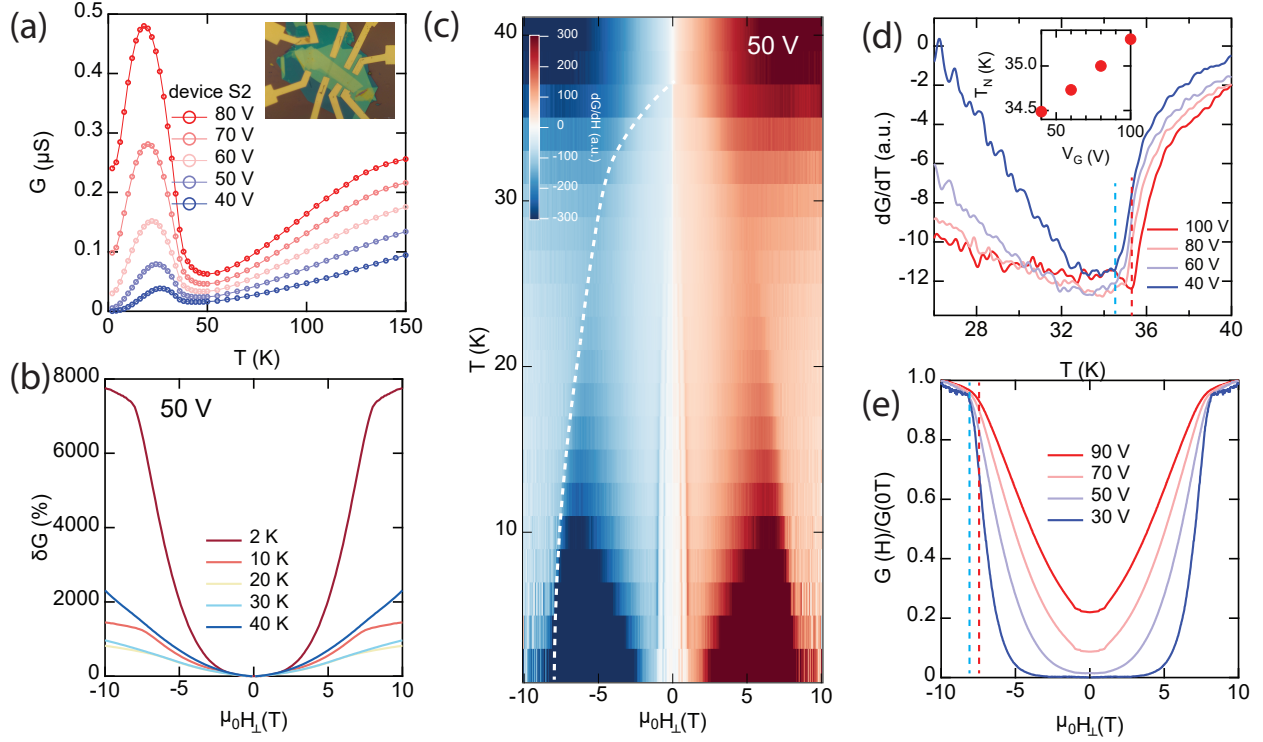


FIG. S5. Low temperature transport measurements on device S2. (a) Temperature dependence of the conductance measured at different gate voltages from +40 to +80 V. (b) Magnetoconductance measured at fixed  $V_G = +50$  V for different temperatures. (c) Color plot of  $dG/dH$  as a function of applied magnetic field and temperature (the white dashed line represent the phase boundary determined by the spin flip transitions). (d)  $dG/dT$  as a function of temperature for different gate voltages. The red and blue dashed line represent the *Néel* transition temperature for +100 and +40 V respectively. The inset shows the *Néel* temperature as a function of applied gate voltages, where a shift of 0.8 K can be clearly seen from +40 to +100 V. (e)  $G(H)/G(0\text{ T})$  as a function of applied magnetic field for  $V_G$  varies from +30 to +90 V (the magnetic field is applied perpendicularly to the layers). The spin flip transition field shifts by approximately 0.5 T from +30 to +90 V.

$T_N$  is shifted by about 0.8 K in device S2, as the backgate voltage is varied from +40 to +100 V. The spin-flip transition and the magnetoconductance are also gate tunable, with magnitude comparable to what we observed on the device we discussed in the main text (see Fig. S5e).

- 
- [1] J. Lee, T. Y. Ko, J. H. Kim, H. Bark, B. Kang, S.-G. Jung, T. Park, Z. Lee, S. Ryu, C. Lee, *ACS Nano* **2017**, *11*, 11 10935.
- [2] J. Son, S. Son, P. Park, M. Kim, Z. Tao, J. Oh, T. Lee, S. Lee, J. Kim, K. Zhang, K. Cho, T. Kamiyama, J. H. Lee, K. F. Mak, J. Shan, M. Kim, J.-G. Park, J. Lee, *ACS Nano* **2021**, *15*, 10 16904.
- [3] F. Wu, I. Gutiérrez-Lezama, S. A. López-Paz, M. Gibertini, K. Watanabe, T. Taniguchi, F. O. von Rohr, N. Ubrig, A. F. Morpurgo, *Advanced Materials* **2022**, *34*, 16 2109759.
- [4] E. J. Telford, A. H. Dismukes, R. L. Dudley, R. A. Wiscons, K. Lee, D. G. Chica, M. E. Ziebel, M.-G. Han, J. Yu, S. Shabani, A. Scheie, K. Watanabe, T. Taniguchi, D. Xiao, Y. Zhu, A. N. Pasupathy, C. Nuckolls, X. Zhu, C. R. Dean, X. Roy, *Nature Materials* **2022**, *21*, 7 754.
- [5] D. Lebedev, J. T. Gish, E. S. Garvey, T. K. Stanev, J. Choi, L. Georgopoulos, T. W. Song, H. Y. Park, K. Watanabe, T. Taniguchi, N. P. Stern, V. K. Sangwan, M. C. Hersam, *Advanced Functional Materials* **2023**, *33*, 12 2212568.